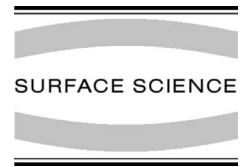




ELSEVIER

Surface Science 482–485 (2001) 1152–1158



www.elsevier.nl/locate/susc

Computer simulated thermal energy atomic scattering on solid surfaces

G. Varga ¹

Department of Physics, Budapest University of Technology and Economics, Budafoki út 8, Budapest H-1111, Hungary

Abstract

Thermal energy atomic scattering on solid surface is investigated by computer simulation. The atomic beam is described by Gaussian wave-packet as an ensemble of independent particles. The atom–solid surface interaction is characterised by an appropriate interaction potential. The interaction potential provides the properties of ideally periodic and disordered surfaces, respectively. The scattering process is governed by time dependent Schrödinger equation that is solved numerically in the case of two-dimensional (2D) and (3D) co-ordinate space. The above-described model provides not only the quantitative intensity distribution but also the animation of the interaction as the time passes. The effect of relative velocity spread, surface disorder and thermal vibration have been investigated efficiently. © 2001 Elsevier Science B.V. All rights reserved.

Keywords: Atom–solid interactions, scattering, diffraction; Computer simulations; Quantum effects

1. Introduction

Thermal energy atomic scattering (TEAS) is a useful tool to investigate the structure, the phonon spectra and the disorder of the solid surfaces [1–4]. The probe particles do not penetrate into the surfaces, the TEAS is non-destructive. TEAS has been treated by an appropriate quantum mechanical model. The atomic beam is described by Gaussian wave-packet as an ensemble of independent particles. The atom–solid surface interaction is characterised by an interaction potential. The applied interaction potential describes the properties of ideally periodic or disordered sur-

faces, respectively. The scattering process is governed by time dependent Schrödinger equation that is solved numerically in the case of two dimensional (2D) and (3D) co-ordinate space [5, 6]. The computations ensure the description of the time propagation of the intensity distribution quantitatively and as an animation, respectively [7].

First of all the resolution of TEAS has been investigated as a function of energy spread of the atomic beam [5]. In the case of ideally periodic surface the resolution of diffraction peaks increases when the energy spread is decreased. This fact proves that the efficiency of the supersonic atomic source is higher than that of an effusive atomic source. Furthermore the transfer width of experimental equipment increases – when the atomic beam monochromaticity is also increased – according to the concept of the transfer width. The

E-mail address: vargag@phy.bme.hu (G. Varga).

¹ <http://goliat.eik.bme.hu/~vargag/> (G. Varga).

relation between the transfer width and the periodicity of the surface topography significantly determines the resolution of the diffraction pattern. The results support the idea that the transfer width has to be significantly greater than the surface period. Otherwise, the resolution of the experiment is not fine enough to determine the exact surface structure.

After that we focused on the scattering from ideally periodic and disordered surfaces [6]. The probability density function (PDF) has been presented in the momentum space. The 2D slices of the ternary PDF parallel to the surface provide the surface topography not only in the case of an ideally periodic surface structure but also in the case of disorder. The computations of He scattering on a model surface have been executed. The periodical and irregularly stepped surfaces have been investigated, too. At last the effect on the thermal vibration of the solid surface was analysed by a simple kinematic model.

2. The physical model

Quantum mechanics basically is able to account for the physical processes of TEAS. In certain conditions – e.g. the probe particles are heavy atoms – semiclassical model approach is appropriate [8,9]. This is the reason we work within the frame of quantum mechanics. The time dependent Schrödinger equation has been applied that corresponds to an initial value problem. This picture provides simple visualisation and physical interpretation. The physical space has been chosen large enough for containing the whole interaction region of TEAS. It means that at the starting-point and at the end-point of the time interval there is no interaction between the particle beam and the solid surface. The wave function remains in the chosen physical space. The incoming atomic beam is described by a plane wave in standard models. The plane wave is an interpretation of an absolutely monoenergetic atomic beam, which has no velocity and energy spread. However, as is known the supersonic atomic beams have a narrow FWHM, because the velocity of the atomic beam may reach few tenfold of local sound velocity. Gaussian wave-

packet provides proper mean velocity and spread of velocity. The Gaussian wave-packet can be considered as a description of an ensemble of neutral atoms with minimised uncertainty in real and momentum space. What does the initial wave packet describe? It describes the collective behaviour of the particles of the atomic beam. The particles of atomic beam does not interact with each other, but they have a special distribution of velocity and energy. The Gaussian wave-packet characterises the atomic beam as a special quantum ensemble of independent particles. For example the 3D Gaussian wave-packet is the following:

$$\begin{aligned} \Psi(x, y, z, t = 0) = C \exp & \left(-(x - x_0)^2 / 2\sigma_1^2 \right. \\ & \left. - (y - y_0)^2 / 2\sigma_2^2 - (z - z_0)^2 / 2\sigma_3^2 \right) \\ & \times \exp(i\mathbf{k}\mathbf{r}), \end{aligned} \quad (1)$$

where Ψ is the wave function, (x, y, z) are the Cartesian co-ordinates, t is the time, C is the normalisation constant, (x_0, y_0, z_0) is the average position at $t = 0$, σ is the standard deviation, i is the complex unit, \mathbf{k} is the wave number vector and \mathbf{r} is the position vector.

Because the present paper focuses on different model calculations of atomic beam scattering; special interaction potentials are applied for describing the interaction between the probe particles and the solid surfaces. The potentials are characterised one by one in Section 4.

3. Numerical method

Let us consider the time dependent Schrödinger equation: $i\hbar \partial\Psi(\mathbf{r}, t)/\partial t = H\Psi(\mathbf{r}, t)$, where \hbar is Planck constant divided by 2π and H is the Hamiltonian. A propagation scheme and an operation of Hamiltonian have to be applied. A splitting operator method has been chosen with third-order accurate formula in time [6]. By splitting the Hamilton operator into two parts, for kinetic energy operator A and potential energy operator B , we receive the exact formal solution: $\Psi(\mathbf{r}, t + \Delta t) = \exp[-i\Delta t(A + B)/\hbar]\Psi(\mathbf{r}, t)$, in the case of time independent potential. This solution is no longer exact for time dependent interaction potential, but ensures efficient time propagation in that case, too.

The above mentioned time propagation can be approximated by an efficient split operator formula, which is a product of operators containing exactly only one of the operators A or B . Our computations have been executed in 2D and 3D Cartesian co-ordinate space. The solution of time dependent Schrödinger equation demands time propagation in every time step and requires a method to determine the effect of Hamilton operator on the wave function. Fast Fourier transformation (FFT) has been applied to calculate $H\Psi$ at every time step, because FFT is an efficient algorithm. FFT is an exponentially convergent approximation of the Hamiltonian and in the momentum space the derivation means simple multiplication.

We have looked for the approximation of $\exp[-i\Delta t(A+B)/\hbar] = \exp[\lambda(A+B)]$ operator by the help of the split formulas. A general decomposition is the following non-symmetric splitting: $\exp(\gamma\lambda A/2) \exp(\gamma\lambda B) \exp[1/2(1-\gamma)\lambda A] \exp[(1-2\gamma)\lambda B] \exp[1/2(1-\gamma)\lambda A] \exp(\gamma\lambda B) \exp(\gamma\lambda A/2)$, where $\gamma = 1/(2-2^{1/3})$. Although this expression involves seven exponential operators, one can show by the computations that the numerical algorithms are more efficient than the algorithms based on the standard second order accurate split operator formula.

To calculate $\exp(\gamma\lambda A/2)\Psi$ it is necessary to work in momentum space where $\exp(\gamma\lambda A/2)$ means a multiplication and a function evaluation. Then we have to go back the real space by an inverse FFT. The calculation of $\exp(\gamma\lambda B)$ means a multiplication and a function evaluation in the real space. The further details of the numerical method can be found in Refs. [5,6].

4. The results

The above described model opens the possibility of computer simulation and dynamical investigation of TEAS. Animations of scattering processes [7] result in direct investigation of the physical phenomenon. In the present work the animations mean snapshots of the PDF in rapid succession. The sequence of the snapshots provides a movie of PDF time evaluation. Obviously, only very few

PDF snapshots of different physical model can be rendered in this paper. One can see the details in Ref. [7]. Below some interesting physical models are discussed.

4.1. Scattering from periodic surface

First of all He–W(112) scattering is demonstrated. 2D Gaussian wave-packet has been chosen as an initial wave function because W(112) has approximately 1D surface corrugation [5]. This is the reason the part of co-ordinate y is left out in Eq. (1).

For describing the interaction the Lennard–Jones–Devonshire type potential has been chosen [10]:

$$V(x, z) = D \exp(-2\alpha z) \left\{ 1 - 2\beta \left[\cos\left(\frac{2\pi}{a}x\right) \right] \right\}, \quad (2)$$

where D is the energy constant, α is the repulsive constant, β is the corrugation constant and a is the lattice constant.

The main data of the computations are the following in Eq. (1) (atomic units (a.u.)): $k_x = 0$, $k_z = -4$, in Eq. (2): $D = 0.00012$, $\alpha = 0.582$, $\beta = 0.2$, $a = 5.18$. Fig. 1 shows the different stages of the PDFs of the scattering in the momentum space when in Eq. (2) (a.u.): $\sigma_1 = \sqrt{5}$, $\sigma_3 = \sqrt{5}$. Fig. 1A and I correspond to the atomic source region and the detector region, respectively. An almost monoenergetic beam can be seen in Fig. 1A. One can see the clear-cut diffraction peaks in Fig. 1I. Fig. 1(B–H) show the propagation of PDF during the scattering.

4.2. The effect of relation between the transfer width and the lattice constant

Now the effect of transfer width on the diffraction pattern is analysed shortly [5]. The concept of the transfer width [11] means the size on the solid surface from that the experimental setup is able to ensure information. Transfer width depends on the energy spread of the atomic beam, the angular spread of the source and of the detector, as well as on the spread of the surface impurity. The above

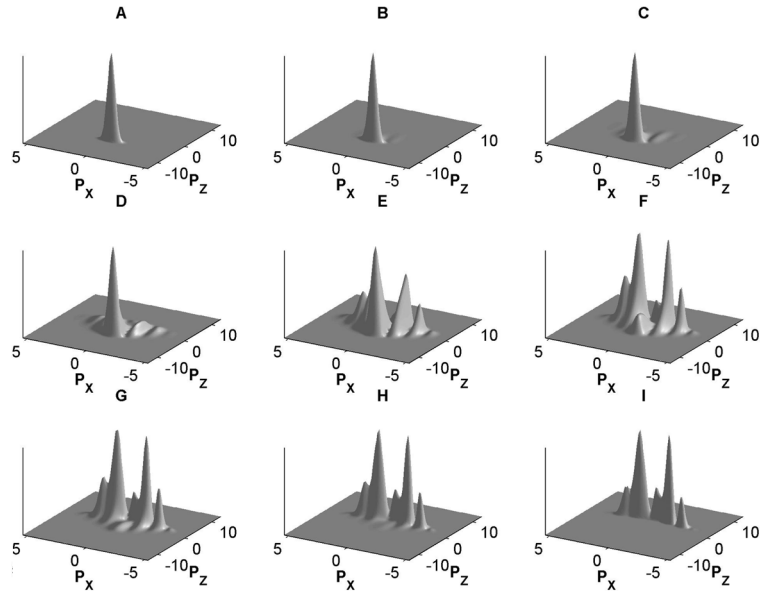


Fig. 1. PDFs of He–W(112) scattering propagation in the momentum space. P_x and P_z are the momenta in direction x and z , respectively. Atomic units are used. (A) PDF is at the beam source region (initial state). (B–H) PDF propagates in the interaction region. (I) PDF is at the detector region (final state).

He–W(112) system is chosen as a starting-point. In this case the relative velocity spread of initial wave function is 5% in both directions (Fig. 2A). Using the same atomic beam the lattice constant is increased in the model computations for exploring the effect on the scattering due to the relation between transfer width and the lattice constant. The resolution is low when the transfer width becomes less than the lattice constant (Fig. 2B, 2C). To verify this connection the relative velocity spread has been chosen significantly less than 5% (Fig. 2D). This means a larger transfer width of the experimental setup. As a result of that the diffraction pattern becomes much more rich, the diffraction peaks do not overlap each other.

4.3. Scattering on irregularly stepped surface

Further computations are executed in the case of He scattering on a typical metal model surface with 2D corrugation function. It demands the solution of 3D time dependent Schrödinger equation. The interaction potential is a Lennard–Jones–Devonshire type:

$$V(x, y, z) = D \exp(-2\alpha(z - \text{disorder}(x, y))) \times \left\{ 1 - 2\beta \left[\cos\left(\frac{2\pi}{a}x\right) + \cos\left(\frac{2\pi}{a}y\right) \right] \right\}, \quad (3)$$

where D is the energy constant, α is the repulsive constant, β is the corrugation constant and a is the lattice constant, $\text{disorder}(x, y)$ ensures the surface disorder.

First of all a completely periodic solid surface was analysed in the case of approximately 30 meV He beam. Input data (a.u.) are in Eq. (1): $x_0 = y_0 = 18.13$, $z_0 = 16.67$, $\sigma_1 = \sigma_2 = \sigma_3 = \sqrt{5}$, $k_x = k_y = 0$, $k_z = -4$, input data (a.u.) in Eq. (2): $D = 0.00012$, $\alpha = 0.582$, $\beta = 0.2$, $a = 5.18$. The $\text{disorder}(x, y) = 0$ and $\text{disorder}(x, y) = 2(\arctan \times (2(y - \max(y)/2)))/(\pi/2) + 1)/2$ correspond to periodic and irregularly stepped surfaces, respectively. Figs. 3 and 4. show the time sequences of PDF in the case of periodic and irregularly stepped surface, respectively. The visualisation of the time evolution is a sophisticated task because the PDF function is a tervariant function. In both cases a parallel slice

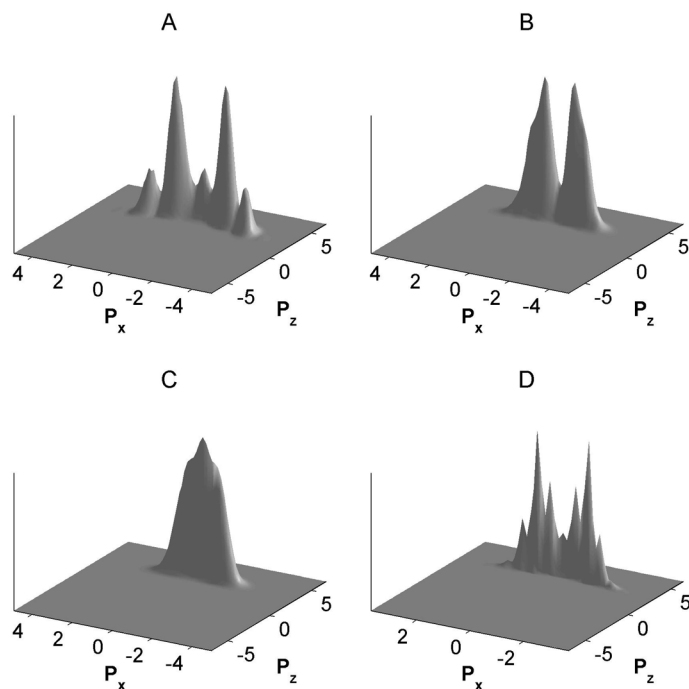


Fig. 2. PDFs in the case of different lattice constants. P_x and P_z are the momenta in direction x and z , respectively. The relative velocity spread of initial wave function is 5% in both directions. (A) Lattice constant is 5.18 (a.u.). (B) Lattice constant is 10 (a.u.). (C) Lattice constant is 13 (a.u.). (D) Lattice constant is 13 (a.u.) but the relative velocity spread of initial wave function is much less than 5% in both directions.

to the surface at the detector region has been chosen. This special slice is called below shortly “window”. This solution resulted 2D images. Both of the figures present a typical series of scattering time propagation. First the Gaussian wave-packet approaches the window and the PDF increases (Fig. 3A–C; Fig. 4A–C). Later on the PDF decreases as the wave-packet goes through the window and it approaches the interaction region of the surface (Fig. 3D; Fig. 4D–E). After the interaction the wave-packet – the He atoms – approaches the window again, but from the reverse direction, from the surface side. The diffraction pattern is propagated (Fig. 3E–I; Fig. 4F–I). The stepped surface leads to a deformed diffraction pattern (Fig. 4) as compared to the case of periodical surface (Fig. 3).

4.4. The effect of thermal vibration

The model contains a time dependent interaction energy that describes the fluctuating surface [12].

The interaction energy is composed of a time independent and a time dependent perturbation part. The time independent part of the interaction energy corresponds to the frozen solid surface. The time dependent interaction energy describes the phenomena of the thermal vibration without energy transfer. There is no energy coupling between the probe particle and the surface in this model. The computations have been executed in the case of time independent and time dependent interaction energy, respectively. The thermal vibration causes a diffuse background of the intensity distribution. This effect changes the intensity pattern. The diffraction peaks overlap each other and their intensities decrease because of the diffuse background.

5. Conclusions

The present work demonstrates that the time dependent Schrödinger equation model is appropriate

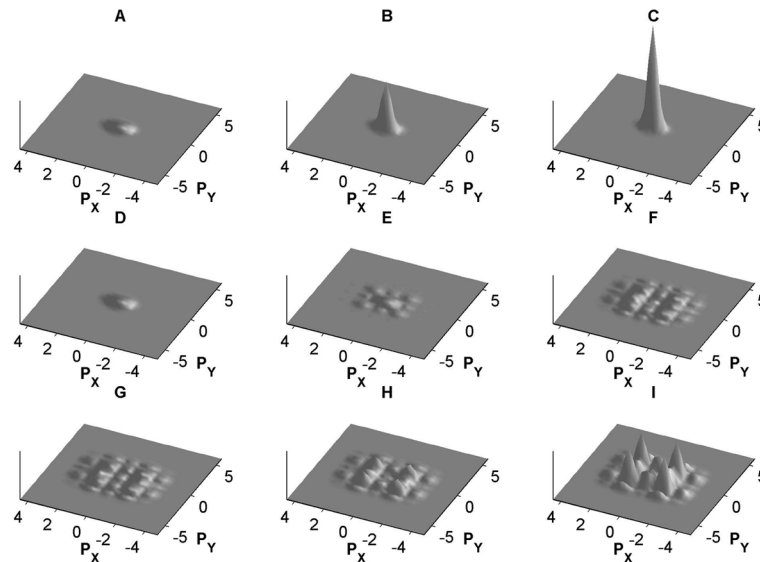


Fig. 3. Slices of the PDFs parallel to the surface in the momentum space as the time elapses in the case of periodical surface at the detector region. P_x and P_y are momenta in the direction x and y , respectively. (A–C) The wave-packet approaches the window (slice) from the atomic source. (D) The wave-packet approaches the surface from the atomic source. (E–I) The wave-packet approaches the window (slice) from the surface. (I) Diffraction pattern in the final state.

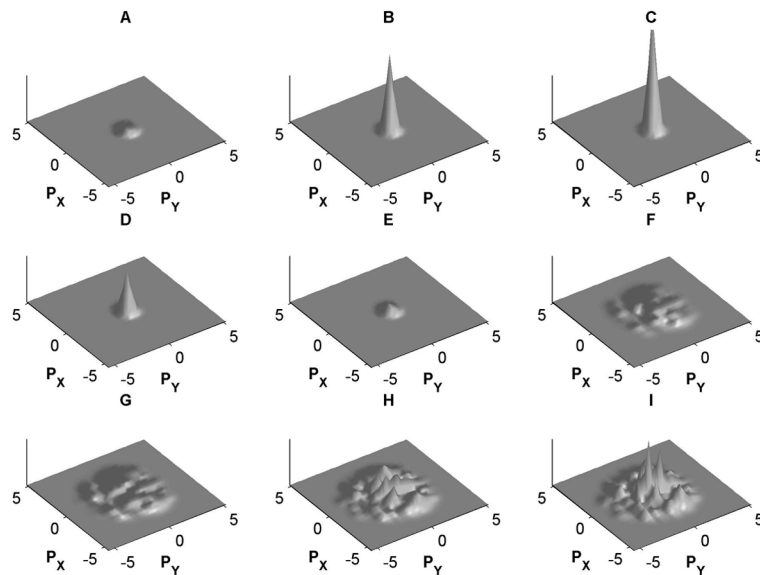


Fig. 4. Slices of the PDFs parallel to the surface in the momentum space as the time elapses in the case of an irregularly stepped surface at the detector region. P_x and P_y are momenta in the direction x and y , respectively. (A–C) The wave-packet approaches the window (slice) from the atomic source. (D–E) The wave-packet approaches the surface from the atomic source. (F–I) The wave-packet approaches the window (slice) from the surface. (I) Diffraction pattern in the final state.

to analyse the TEAS. Simulations of different atom–solid surface systems result in typical time

propagation and structure of the intensity distributions. These properties describe the given

atom–solid surface systems. Comparing the experimental results with the simulation results, the interaction processes can be determined to first order. The computer animation can illustrate the typical physical phenomenon of TEAS. These advantages may provide a useful theoretical tool in the thorough investigation of TEAS. The effectiveness of the animations can be explored by real computer simulation [7].

References

- [1] D. Fariás, K.H. Rieder, *Rep. Prog. Phys.* 61 (1998) 1575–1664.
- [2] G. Comsa, *Surf. Sci.* 299/300 (1994) 77.
- [3] V. Bortolani, A.C. Levi, *Atom Surface Scattering Theory*, Bologna, 1986.
- [4] G. Benedek, U. Valbusa (Eds.), *Dynamics of Gas–Surface Interaction*, Springer, Berlin, 1982.
- [5] G. Varga, *Appl. Surf. Sci.* 144/145 (1999) 64–68.
- [6] G. Varga, *Surf. Sci.* 441 (1999) 472–478.
- [7] G. Varga, Home Page, Scattering animations (2000): <http://goliat.eik.bme.hu/~vargag/>.
- [8] B. Gumhalter, K. Burke, D.C. Langreth, On the Validity of the Trajectory Approximation in Quasi-adiabatic Atom–Surface Scattering, 3S Symposium on Surface Science, Obertraun, Austria, 1991.
- [9] G. Varga, Seventh Vacuum Conference, Budapest, Hungary, Extended Abstracts, 1997, p. 234.
- [10] A.T. Yinnon, R. Kosloff, *Chem. Phys. Lett.* 102 (1983) 216.
- [11] G. Comsa, *Surf. Sci.* 81 (1979) 57.
- [12] G. Varga, E. Balázs, L. Füstöss, Effect of thermal vibration of He scattering on solid surface, Eighth Joint Vacuum Conference 2000, Pula, Croatia.